Three-dimensional spectral measurements of paint samples using optical coherence tomography

Maria, Michael; d'Hont, Lieve; Anisimov, Andrei G.; Stols-Witlox, Maartje; Groves, Roger M.

DOI
10.1117/12.2592663

Publication date
2021

Document Version
Final published version

Published in
Optics for Arts, Architecture, and Archaeology VIII

Three-dimensional spectral measurements of paint samples using optical coherence tomography

Maria, Michael, d'Hont, Lieve, Anisimov, Andrei, Stols-Witlox, Maartje, Groves, Roger

Michael Maria, Lieve d'Hont, Andrei Anisimov, Maartje Stols-Witlox, Roger Groves, "Three-dimensional spectral measurements of paint samples using optical coherence tomography," Proc. SPIE 11784, Optics for Arts, Architecture, and Archaeology VIII, 117840Q (8 July 2021); doi: 10.1117/12.2592663

Event: SPIE Optical Metrology, 2021, Online Only

Three-dimensional spectral measurements of paint samples using optical coherence tomography

Michael Maria*[a], Lieve d'Hont[b], Andrei G. Anisimov[a], Maartje Stols-Witlox[b] and Roger M. Groves[a]
[a]Structural Integrity and Composites, Faculty of Aerospace Engineering, Delft University of Technology, Kluyverweg 1, 2629 HS Delft, The Netherlands
[b]Conservation & Restoration, University of Amsterdam, Johannes Vermeerplein 1, 1071 DV Amsterdam, The Netherlands
*m.maria-1@tudelft.nl

ABSTRACT

In this study, we describe a method for measuring the spectral reflectance of a paint layer at both the surface and in the volume of the paint layers. We first present a fringes model which illustrates the possibilities for spectral reconstruction using a Short-Time-Fourier-Transform algorithm. We investigate the remaing percentage errors and identified that there is a strong fluctuation along the wavelength range of the spectrometer. Then, we demonstrate the validity of our approach experimentally by measuring the spectral reflectance of a paint layer using a custom-made visible light optical coherence tomography system. There, we reconstruct the spectral reflectance of a paint layer by probing the surface and a depth range below the surface. Finally, we show the importance to include a wavelength sensitive correction in the reconstruction for taking into account the spectral shape of the light in the reference path of the interferometer. This work is part of the Down To The Ground project, in which the results of the OCT inspection will be used directly by a consortium of technical art historians and conservators.

Keywords: Optical Coherence Tomography, Hyperspectral Imaging, Spectroscopy, Spectral Calibration

1. INTRODUCTION

Identifying paints and pigments using spectral imaging techniques is a common approach in cultural heritage preservation science [1,2]. More particularly, Hyperspectral Imaging (HSI) offers the possibility to characterise the distribution of pigments over a region of interest with relative high-speed and high sensitivity. However, the main limitation of HSI in this context is that it is spatially a two-dimensional technique [3]. In other words, the information provided by HSI is given as a two-dimensional mapping of the object's reflectance with no separate access to the contribution of each layers.

Optical Coherence Tomography (OCT) is an imaging technique that can obtain a three-dimensional structural representation of a semi-transparent object with high-spatial resolution. Traditionally, OCT is used to provide structural spatial information. However, a recent approach based on spectroscopy concepts have investigated the feasibility of using OCT for spectral imaging [4,5,6]. The key here is to use an algorithm similar to the Short-Time-Fourier-Transformation (STFT) to analyse the interference fringes with spectral selectivity.

In this paper, we present the work conducted to measure the spectral reflectance of a paint layer from its surface and from within the layer itself. Using a fringes model and experimental data measured using our custom visible light OCT system, we are able to demonstrate a relatively accurate reconstruction of the spectral reflectance from both the surface and form within the paint layer. This work is part of the Down To The Ground project [7], in which the results of the OCT inspection will be used directly by a consortium of technical art historians and conservators.

2. FRINGES MODEL AND STFT

The signal detected by a spectrometer in an SD-OCT system can be approximated, after basic correction (dark signal and background correction), as in [8]

Optics for Arts, Architecture, and Archaeology VIII, edited by Haida Liang, Roger Groves, Proc. of SPIE Vol. 11784, 117840Q · © 2021 SPIE · CCC code: 0277-786X/21/$21 · doi: 10.1117/12.2592663

$$I(\lambda) \propto 2\sqrt{I_S(\lambda) I_R(\lambda)} \cos\left(\frac{2\pi}{\lambda} \times 2z_0\right), \tag{1}$$

where $I(\lambda)$, $I_S(\lambda)$ and $I_R(\lambda)$ are the optical intensities corresponding to the total signal, the sample path of the interferometer only and the reference path of the interferometer only, λ is the wavelength of the light and z_0 is the position in depth of a flat mirror acting in this situation as the sample.

Through the Fourier Transform operator, Equation 1 leads to,

$$I(z) \propto \mathrm{FT}\left[I(\lambda)\right] = 2\sqrt{I_S(\lambda) I_R(\lambda)} \times \delta(z \pm 2z_0) \tag{2}$$

where I(z) is the axial scan (A-scan) representing the depth reflectivity profile of the situation described by Equation 1 and $\delta(z \pm 2z_0)$ is a Dirac function. Building on Equation 2, the optical intensity corresponding to the sample path of the interferometer only and hence the spectral reflectivity of the sample can be inferred as,

$$I_S(\lambda) \propto \frac{I(z)^2}{4I_R(\lambda)}. \tag{3}$$

Equation 3 is obtained by applying a Fourier-Transform operation onto the entire spectral range detected by the spectrometer. Doing so and applying a classical OCT approach, this will lead to a relatively high axial resolution in the structural imaging mode. However, considering the time-bandwidth constraint, no meaningful spectral information can be extracted. Therefore, to obtain spectral information, one needs to apply a filter to the original signal detected by the spectrometer. This is done by multiplying the signal $I(\lambda)$ by a window filter $W_i(\lambda)$ and selecting a given spectral range characterised by its central wavelength $\lambda_{c,i}$ and bandwidth $\Delta\lambda_i$. The central wavelength and the spectral width of each window are adjusted in order to maintain the axial resolution and allow a direct signal-to-noise ratio (SNR) comparison possible between intensity within A-scans.

$$W_i(\lambda) = \frac{1}{\Delta\lambda_i \sqrt{2\pi}} \exp\left[-\frac{(\lambda - \lambda_{c,i})^2}{2\Delta\lambda_i^2}\right] \tag{4}$$

Figure 1 is an illustration of the results obtained using the model above. While simple, it shows that this model is already enough to understand some of the concepts involved in extracting spectral information from low-coherence interferometry data. Figure 1(a) shows the interference fringes obtained from particular reference-path and sample-path signals. The intensity fluctuations observable superposed on the fringes are caused by intensity noise which is including in the model following the approach of Jensen and al. [9] by considering for the example of Figure 1 an integration time of 10 µs, a light source repetition rate of 250 kHz and a light source pulse length of 1 ns. Figure 1(b) is the reconstruction which is achieved using Equation 3. The black line represents the reconstruction obtained without dividing by the reference path signal. This correction is necessary if there are significant variations of the reference path signal amplitude throughout the spectral range. Because of the intensity noise within the system, there is a random error remaining in the reconstruction. Figure 1(c) shows the amplitude of the error along with the spectral range. For this situation characterised by a critical intensity noise level in the system (integration time of 10 µs) [9], the error peaks at around 30 % with an average error of 10 %. When the intensity noise level within the signal decreases, the error (statistical mean of the averaged spectral error) drops significantly and flattens at around 1 %. This remaining error is certainly caused by imperfect detection (minimal intensity noise level corresponding to shot noise).

2.1 Visible Optical Coherence Tomography system

In order to validate the findings obtained using the fringes model, a custom-made OCT system using visible light has been used. The system uses a supercontinuum light source (Electro VISIR- Leukos (France)) filtered to illuminate the interferometer with visible light, for wavelengths from around 450 nm up to 700nm. The interferometer is a Michelson interferometer built from bulk optical components. Finally, the spectrometer is a commercial spectrometer (COBRA VIS – Wasatch Photonics (United States)) sensitive from 500 nm to 700 nm range. The multiple active components are interfaced through LabView 2020 and the data are processed using custom-made algorithms using Matlab 2020. The system is sketched in Figure 2.

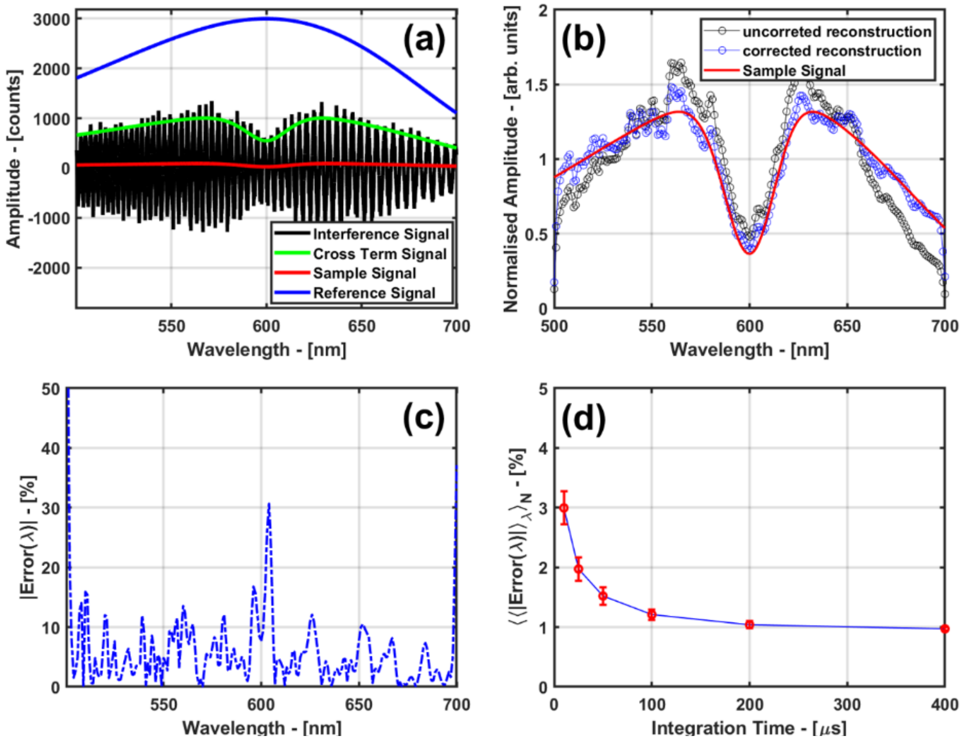

Figure 1: Summary of results obtained using the fringes model. (a) Examples of spectra and fringes pattern, (b) Example of reconstructed spectra, (c) Representation of the wavelength-dependent error between reconstructed spectra and ground truth and (d) Variation of the error with the intensity noise level.

3. EXPERIMENTAL RESULTS

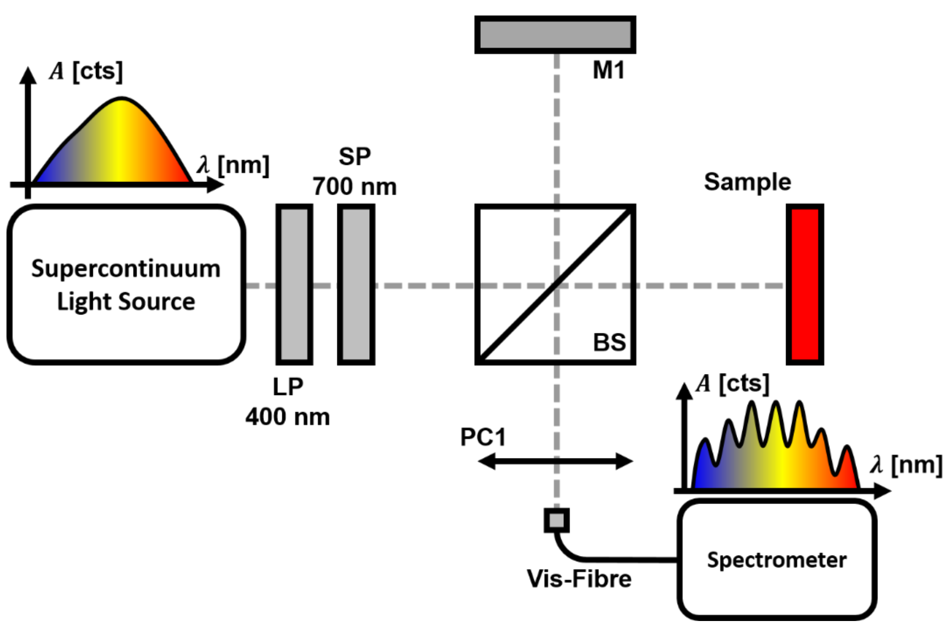

Figure 2: Schematic representation of the Vis-OCT system. LP: Long Pass filter, SP: Short Pass filter, BS: Beam Splitter, M1: Flat Mirror, PC1: Parabolic Collimator, Vis-Fiber: Optical Fiber for visible light and A is the signal amplitude.

3.1 Reflectivity measurements

As mentioned above, the STFT approach is an interesting way to obtain spectral information from a low-coherence interferometry system such as the one used in OCT. To demonstrate the usefulness of this approach in 3D spectral measurement, we show below the results obtained while imaging a paint layer [10]. Figure 3(a) shows as an example the result of the windowing process for central wavelengths of 500 nm, 505 nm and 690 nm. The bandwidth of each window is adjusted to maintain an axial resolution, for comparison of SNR, of 50 µm (corresponding to a spectral resolution in the range of a few nanometres for all three central wavelengths). The three resulting A-scans obtained from the windows of Figure 3(a) are displayed in Figure 3(b). The peaks corresponding to the paint surface can be observed at a depth of around 0.075 mm. Using the STFT algorithm, two techniques are used to reconstruct the sample's spectral reflectance profile. The first one, denoted Max-based on Figure 3(c-d), relies on tracking the maximum of each A-scan (obtained for each spectral window W(λ)). The second one, denoted Avg-based on Figure 3(c-d), calculates an average value of the A-scan signals considering a specific depth range. In Figure 3(c-d), the depth range considered is 83 µm to 89 µm (in air). From these reconstructed spectra, it appears that the second approach (average-based) offers a better result (closer to the expected spectral reflectance of a red paint layer [11]). The main reason for this difference between surface-based and depth-based approach is, we believe, the roughness of the paint. Low coherence interferometry relies on backscattering signals which are more often than not weak (µW) compared to the optical power of the illumination (mW). However, because of the random roughness pattern of the paint layer, it can happen that the reflected signal consists of a significant portion of specular reflection, which has an optical power that is quite comparable to that of the illumination one (100s µW to mW). Also, the importance of correcting for the reference signal spectral shape is demonstrated here from Figure 3(c) to Figure 3(d). Without correction, the lower spectral range shows an overestimated reflectance. However small, this correction may have a significant impact on the ability to detect fine spectral variations in future experiments.

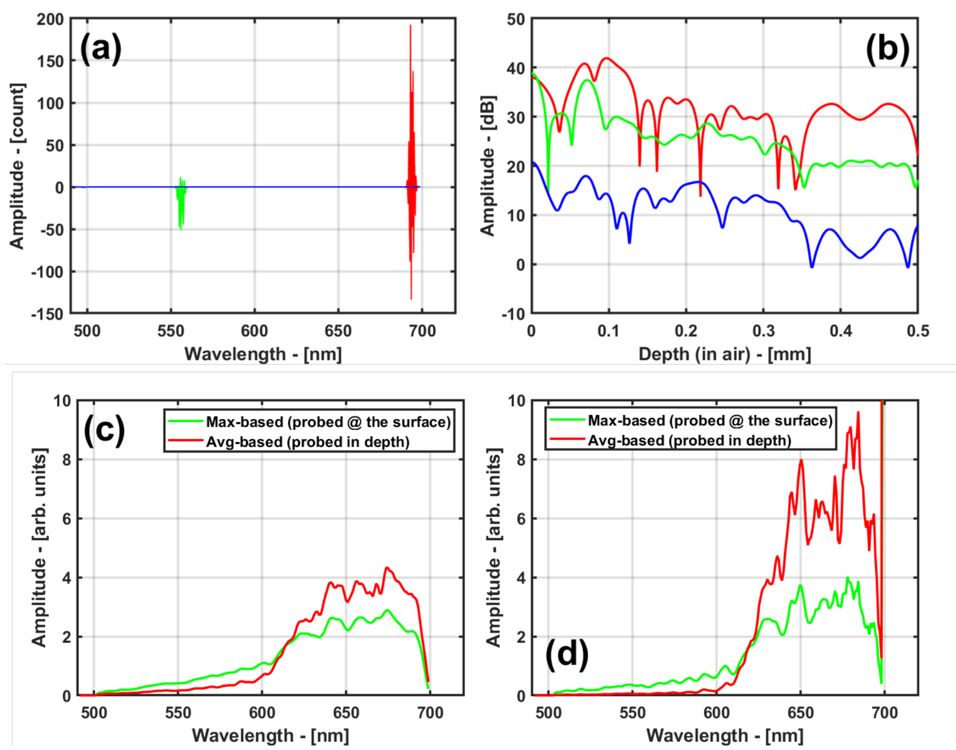

Figure 3: Illustration of experimental STFT algorithm for reconstruction of spectral reflectance of a paint layer (red). (a) Example of spectra after windowing, (b) Corresponding A-scan obtained after STFT, (c) Spectra obtained after non-corrected reconstruction and (d) Spectra obtained after correction.

4. CONCLUSION AND FUTURE WORK

This paper describes through a simple fringes model and some experiments the path towards measuring the volumetric spectral reflectance of an object in three dimensions using OCT. Our study shows that the STFT is a suitable approach for that problem. However, some limitations such as chromatic effects or intensity noise need to be accounted for to obtain accurate spectral reconstruction. We show a relatively precise reconstruction of a paint layer (red) based on a surface measurement and in-depth measurements in the paper. Our future work includes some investigations on the chromaticity of the system to allow for large-scale spatial averaging, particularly useful in the field of cultural heritage. Also, we will look into the intensity noise effect and compensation to minimise the error on the reconstruction.

5. ACKNOWLEDGMENT

This work is supported by the Dutch Research Council (NWO) through the project *Down To The Ground*: *A Historical, Visual and Scientific Analysis of Coloured Grounds in Netherlandish Paintings, 1550-1650* (VC.GW17.029).

REFERENCES

[1] Liang, H., "Advances in multispectral and hyperspectral imaging for archaeology and art conservation," *Appl. Phys. A* 106, 309–323 (2012). https://doi.org/10.1007/s00339-011-6689-1

[2] Balas, C., Epitropou, G., Tsapras, A., Hadjinicolaou, N., "Hyperspectral imaging and spectral classification for pigment identification and mapping in paintings by El Greco and his workshop," *Multimed Tools Appl* **77,** 9737–9751 (2018). https://doi.org/10.1007/s11042-017-5564-2

[3] Delaney, J.K., Dooley, K.A., Radpour, R., Kakoulli, I., "Macroscale multimodal imaging reveals ancient painting production technology and the vogue in Greco-Roman Egypt," *Sci Rep* 7, 15509 (2017). https://doi.org/10.1038/s41598-017-15743-5

[4] Rubinoff, I., Kuranov, R.V., and Zhang, H.F. "Intrinsic spectrally-dependent background in spectroscopic visible-light optical coherence tomography," *Biomed. Opt. Express* 12, 110-124 (2021).

[5] Robles, F., Wilson, C., Grant, G., Wax, A., "Molecular imaging true-colour spectroscopic optical coherence tomography," *Nature Photon* 5, 744–747 (2011). https://doi.org/10.1038/nphoton.2011.257

[6] Harper, D.J., Konegger, T., Augustin, M., Schützenberger, K., Eugui, P., Lichtenegger. A., Merkle, C.W., Hitzenberger, C.K., Glösmann, M., Baumann, B., "Hyperspectral optical coherence tomography for in vivo visualization of melanin in the retinal pigment epithelium," *J. Biophotonics.* 2019;12(12):e201900153. doi:10.1002/jbio.201900153

[7] Maartje Stols-Witlox, “Down To The Ground”, University of Amsterdam, https://ahm.uva.nl/content/projects/down-to-the-ground/down-to-the-ground.html (May, 2021).

[8] Izatt J.A., Choma M.A. (2008) Theory of Optical Coherence Tomography. In: Drexler W., Fujimoto J.G. (eds) Optical Coherence Tomography. Biological and Medical Physics, Biomedical Engineering. Springer, Berlin, Heidelberg. https://doi.org/10.1007/978-3-540-77550-8_2

[9] Jensen, M., Gonzalo, I.B., Engelsholm, R.D., Maria, M., Israelsen, N.M., Podoleanu, A. and Bang, O., "Noise of supercontinuum sources in spectral domain optical coherence tomography," *J. Opt. Soc. Am. B* 36, A154-A160 (2019).

[10] Old-Holland Classic Oil Colours, Madder (Crimson) Lake Deep Extra (PR83 Dihydroxy Anthraquinone), bought in 2019, applied with a brush in October 2020 to the white area of a LENETA FORM 2A Opacity chart.

[11] Maria, M., Anisimov, A.G., Stols-Witlox, M. and M. Groves, R.M., "Analysis of a SD-OCT-based hyperspectral system for spectral reflectance measurements", Proc. SPIE 11354, Optical Sensing and Detection VI, 113541J (1 April 2020); https://doi.org/10.1117/12.2555435